

**Fabrication of
Transparent Conductive Oxide Thin Films
in the In-Ga-Zn-O and In-Sn-Zn-O Systems
by Facing-Target DC-sputtering Technique**
(対向ターゲット式DCスパッタリング法によるIn-Ga-Zn-O
およびIn-Sn-Zn-O系透明導電性酸化物薄膜の作製)

XINZHI WANG

Doctoral Thesis



**Department of Chemical Science and Technology,
Graduate School of Advanced Technology and Science,**

TOKUSHIMA UNIVERSITY

2017

**Fabrication of
Transparent Conductive Oxide Thin Films
in the In-Ga-Zn-O and In-Sn-Zn-O Systems
by Facing-Target DC-Sputtering Technique**

**A THESIS SUBMITTED FOR THE DEGREE OF DOCTOR
OF PHILOSOPHY**

**By
XINZHI WANG**

Supervisor: Prof. Toshihiro MORIGA

**Department of Chemical Science and Technology,
Graduate School of Advanced Technology and Science,**

**TOKUSHIMA UNIVERSITY
2017**

Outline

Outline.....	- I -
Chapter 1: Introduction of Transparent Conductive Oxides	- 1 -
§1.1 Foreword.....	-1-
§1.2 Research status of Transparent Conductive Oxides.....	-2-
§1.3 Introduction of Facing-Target DC-sputtering Technique.....	-8-
§1.4 Research Topics and Contents.....	-12-
Chapter 2: Processes of Transparent Conductive Oxides.....	- 14-
§2.1 Raw Material.....	- 14 -
§2.2 Experimental Instruments.....	- 15 -
§2.3 Experimental Processes.....	- 15 -
§2.4 Material Characterization.....	-15 -
Chapter 3: Experimental Research on In-Ga-Zn-O Material.....	- 17-
§3.1 In-Ga-Zn-O thin films by DC magnetic sputtering.....	- 17 -
§3.2. Material Characterization.....	- 17 -
§3.3. Brief Summary.....	-22 -
Chapter 4 : Experimental Research on In-Sn-Zn-O Material.....	- 23-
§4.1. In-Sn-Zn-O thin films by DC magnetic sputtering.....	- 23 -
§4.2. Material Characterization.....	-23 -
§4.3.Brief Summary.....	- 27-
Chapter 5: Conclusions and future works	-28 -
§5.1. Summary and Conclusions.....	-28 -
§5.2. Suggestion for future works.....	-28-
References.....	-29-
Appendix: Section of CASTEP calculations.....	32-

Acknowledgements.....	-42-
Biography.....	-43-
Publication list.....	-44-

Chapter 1: Introduction to Transparent Conductive Oxides

§1.1 Foreword

Transparent conductive oxide films display high visible light transmittance and high conductivity and hence have a wide range of applications in the field of electronics. The specific performance requirements of transparent conductive oxides are as follows: an average transmittance of higher than 80% in the average visible light range ($\lambda = 380\text{--}760\text{ nm}$), and a resistivity below $10^{-3}\ \Omega\cdot\text{cm}$.^[1] These properties appear to be contradictory; to ensure that the material has the required conductivity, it must make the center of the Fermi sphere deviation from the momentum space origin, in accordance with the band theory of solids. If the energy levels are densely distributed, the energy levels are occupied by electrons and the energy gap is very small, so that when light is incident upon the material, the photoelectric effect is easily produced. Therefore, the production of an internal photoelectric effect adversely affects light transmittance. The forbidden band width must be greater than the photon energy. For a wide band gap transparent conductive oxide semiconductor to maintain good visible light transmission, the plasma frequency must be less than the visible frequency, and to maintain a specific conductivity, a specific carrier concentration is required; therefore, the ion frequency and carrier concentration must be in defined proportions.^[2]

This section introduces the application and development of common transparent conductive films, including traditional transparent conductive oxide films, p-type transparent conductive oxide films, novel flexible transparent conductive films, and transparent electronic devices. The progress of research into transparent conductive mechanisms and the preparation processes of transparent conductive films are discussed in detail, and the research and application prospects of transparent conductive films are briefly discussed. Transparent conductive oxide films have a wide range of applications in the field of electronics, such as in solar cells, displays, gas sensors, antistatic coatings, semiconductor/insulator/semiconductor (SIS) heterojunctions, modern fighters, and cruise missile window materials.^[3, 4, 5] Due to the excellent photoelectric properties of transparent conductive oxide films, they have

been developed rapidly in recent years, especially in flat-panel LCD, thin film transistors (TFT), solar cell transparent electrodes, infrared radiation reflection mirror coatings, trains and aircrafts with glass defrost, curtain wall glass, and a wide range of other applications.

§1.2 Research status of Transparent Conductive Oxides.

In_2O_3 materials possess a body-centered cubic crystal structure, and a forbidden band width of 3.75–4.0 eV, with good light transmission. Owing to the large amount of oxygen vacancy defects that occur during the preparation of In_2O_3 -based thin films, there are excess free electrons, resulting in electrical conductivity. ITO, the most widely used TCO (Transparent Conductive Oxides) film, is currently the most popular research subject. ITO film has a band gap width of 3.5–4.25 eV, a carrier concentration of 10^{20} cm^{-3} , an electron mobility of 10 to $30 \text{ cm}^2 / (\text{V}\cdot\text{s})$, and a resistivity of about $5 \times 10^{-4} \Omega\cdot\text{cm}$. Up to $5 \times 10^{-5} \Omega\cdot\text{cm}$ is close to most metal resistivity. Its infrared reflectance at $10 \mu\text{m}$ can be as high as 80%. In addition, it has high hardness; chemical resistance; and excellent performance in integrated circuits, intelligent transportation, and energy-saving buildings. It has been regarded as the preferred material for practical TCO films in a wide range of applications.^[6]

There are many methods for the preparation of ITO films,^[7] including magnetron sputtering (direct current magnetron sputtering (DCMS) and radio frequency magnetron sputtering (RFMS)), vacuum evaporation, atomic layer deposition, pulsed-laser deposition, sol-gel, spray pyrolysis, and chemical vapor phase deposition. Among these, magnetron sputtering, sol-gel and spray thermal decomposition are the most widely used for commercial applications. At present, the magnetron sputtering method is the most commonly used coating technology, and is used in a large-scale production line manufacturing process. Basic research on the ITO film is mainly focused on its mechanism and performance, the preparation of ITO on a flexible substrate, and the development of its field of application.

SnO_2 is a direct band gap, wide band gap oxide semiconductor with a band gap of 3.5–4.0 eV, a resistivity of 10^{-4} – $10^6 \Omega\cdot\text{cm}$ and a carrier concentration of up to 10^{20} cm^{-3} . It has a regular tetrahedral rutile structure; good transmittance, conductivity,

chemical stability, and adsorption; can be deposited on glass, ceramics and other substrate materials; and also displays reflective infrared radiation shading. The advantages of SnO₂ films are that they are made from widely available resources, are not expensive, and are non-toxic. Enabling their use in liquid crystal displays, solar photovoltaic cells, gas sensors and other fields, such as in energy-saving windows and other large-scale building materials. Therefore, SnO₂-based transparent conductive films are of interest to many researchers. [8] The doping of high-conductivity SnO₂ films has been a widely researched topic. Among all the dopant elements, F is the most versatile and widely used element with the best doping effect. FTO film resistivity is about $1 \times 10^{-4} \Omega \cdot \text{cm}$ and its visible light transmittance is 80% or more. FTO film is widely used in flat panel display devices, solar cells, electric heating panels, touches screens and other devices, and has been applied abroad in the commercialization of radiant glass film. Electrochemical cyclotron resonance chemical vapor deposition (ECRCVD), laser pulse deposition, sol-gel, and electrostatic spray vapor deposition (electrostatic spraying) methods have been studied using chemical vapor deposition, electron cyclotron resonance, metal-organic vapor deposition, enhanced soaking and vapor deposition (ESVD), and reactive sputtering. The current research into FTO films is mainly focused on its conductivity, improvement of the preparation process, preparation of a large film area, and the expansion of the application field.

ZnO is a direct band gap, wide band gap, and n-type semiconductor material with a hexagonal wurtzite structure of group II-VI. The band gap of ZnO is about 3.37 eV at room temperature and its melting point is 1975 °C, so it has high thermal and chemical stability. [6] Moreover, ZnO thin films have a favorable epitaxial growth temperature, which can reduce the equipment cost, inhibit the diffusion of the solid phase, and improve the film quality. Doping of ZnO is rich, inexpensive, and non-toxic, with excellent overall performance, and so it has become of interest in semiconductor optoelectronic materials research throughout the international community. Since the 1980s, the study of doped ZnO has rapidly advanced. [9, 10, 11, 12.]

With continuous improvements to the film and doping process, its performance is

gradually approaching that of ITO. Compared with ITO thin films, ZnO thin films have the advantages of low cost, abundant resources, non-toxicity and relatively low deposition temperatures, and hence, they are considered to be the most promising materials for the replacement of ITO (Indium Tin Oxide). Additionally, because of the deterioration of the optical properties of SnO₂ in a hydrogen plasma atmosphere, its application as a transparent pre-conductive electrode in a microcrystalline silicon solar cell is limited, whereas the characteristics of ZnO are resistant to hydrogen plasma radiation, enabling its use in this particular application. The ZnO/Al (AZO) thin films are the most promising.^[13]

ZnO-based thin films have a resistivity of up to $1.4 \times 10^{-4} \Omega \text{cm}$ and visible light transmittance of more than 80%. AZO film has low resistivity, high visible light transmittance, and high infrared reflectivity, and can therefore meet the requirements of related electronic devices and equipment. However, more advances are required for its application in high-performance optoelectronic devices. Most of the research into application of this material is mainly in the developmental stages; currently, only solar cells can be produced industrially. At present, research into the AZO transparent conductive film is mainly focused on the optimal process parameters of various preparation methods for obtaining high quality AZO thin films with low resistivity, high transmittance, high crystal quality, good adhesion with the substrate; the conductive mechanism; and exploring the best conditions for industrial growth. Although the preparation process of the AZO film is difficult to control, resulting in a lack of product uniformity, stability, and repeatability, we believe that with further research, AZO films are likely to become the next generation of transparent conductive films.

Indium gallium zinc oxide (IGZO) is a new material used in the generation of thin film transistor liquid crystal displays.^[14] At the end of 2004, Prof. Hideo Hosono, a professor at the Tokyo University of Technology, reported that an amorphous oxide semiconductor (AOS) with the composition a-InGaZnO₄ (a-IGZO) can be used in the manufacturing of flexible thin film transistors. Transparent thin film transistors (TFTs) show significantly improved performance compared to conventional TFTs based on a-

Si: H (hydrogenated amorphous silicon) and organic materials. AOS materials have enhanced properties compared to traditional semiconductors, so AOS TFT technology leading towards the production of flat panel displays is developing very rapidly. ^[15] Various prototyped active matrix displays (digital displays) have been developed by several companies over the past five years since the first AOS thin film transistor was reported. In the original paper, the characteristics of the AOS material relating to its TFT characteristics were analyzed; focusing on the reason the specific electronic structure of the transparent oxide can cause the AOS to have such attractive electrical properties. The first AOS TFT was reported at the end of 2004. In 2005, letterpress printing followed the first black and white electronic paper using a-IGZO TFT, which is an active matrix display based on AOS. In 2006, the Relief was developed with full-color electronic paper, using an advanced "front drive" structure in which a transparent a-IGZO TFT color filter array and a TFT array were used on the front panel. ^[16] Current electronic paper technology can produce flexible black and white electronic paper of size 5.35 in and resolution of 150 pixels/in (ppi); the highest resolution of 400 ppi can be achieved for 2 in flexible black and white electronic paper. Full color electronic paper of size 5.35 in and resolution of quarter video graphics array (QVGA, 320 x 240 pixels) can be achieved using the front drive structure. In 2006, LG Electronics reported the first active organic light emitting diode (AMOLED) display, which resulted in the development of a flexible OLED made of stainless steel foil in 2007. At the April 2008 International Conference on Information Display, Samsung reported a new AMOLED display, the sector's largest AMOLED display at 12.1 in, with a working frequency of 240 Hz, apply to the 15-in LCD. Sharp, in cooperation with the Japan Semiconductor Energy Research Institute, announced on June 1, 2012, the development of a crystalline, improved performance of a new IGZO-TFT that could be used in smart phones and tablet terminals, etc. to promote high-precision LCD panels and organic EL panel drive components. At a press conference held in Tokyo on June 1, Sharp unveiled liquid crystal panels and organic electro-luminescence (OEL) panels with IGZO TFT, which developed the IGZO TFT further. There were two liquid crystal panels of 4.9 in and 6.1 in, respectively, with pixel and resolution aspects of 1280 × 720 pixels, 302 ppi resolution, for the 4.9-in

product, and 2560×1600 pixels, 498 ppi resolution, for the 6.1-in product. The OEL panels were 13.5 in and 3.4 in, with pixels ranging from 3840×2160 pixels and 960×540 pixels and a resolution of 326 ppi.

Canon developed a faster fifth-order ring oscillator using a-IGZO TFTs, demonstrating 410 kHz oscillations, with dynamic characteristics that were shown to be consistent with the static characteristics. At present, the fastest AOS ring oscillator, reported by the Samsung Advanced Technology Research Institute, has a 0.94 ns delay per order. Canon also exhibited OLED pixels that drive a frame rate of 120 Hz. The team at the Brunswick University of Technology in Germany demonstrated the use of transparent OLED pixels using Zn-Sn-O (a-ZTO) TFTs. The National Taiwan University research team conducted research into flexible integrated circuits, and reported a-IGZO TFT-based flexible fifth-order ring oscillator for the first time.

Over the past few decades, n-type electronically conductive TCO films have been thriving, but their applications are limited to a single electrical coating or optical coating of passive devices, making production of true "transparent devices" difficult. The reason for this is the lack of good photoelectric properties of p-type hole conductive TCO film material. The existing p-type TCO conductivity is very different from that of the n-type TCO; p-type TCO films typically have a lower conductivity by 3-4 orders of magnitude, and lower visible light transmittance, restricting the transparent pn junction, transparent thin film transistor (TTFT), and hence the implementation of full transparent active devices.

The main reason for the lack of p-type TCO material is that the oxygen ions in the oxide have great electronegativity, and the valence band of the oxide has a strong localization effect on the hole, i.e., the 2p level of the O is often much lower than that of the metal atomic valence band. Therefore, a lot of energy is needed to overcome the oxygen ion barrier on the hole. The early p-type transparent conductive films were mainly composed of Cu^{2+} , which weakens the effect of oxygen ion electronegativity on the localization of holes. After the 1990s, p-type conductive NiO: Li thin films were reported, and p-type CuAlO_2 films were prepared by valence band chemical modification. NiO is the first material to be used for p-type doped oxides. In 2015, the

preparations of nickel oxide film and device performance were studied under different oxygen partial pressures. CuAlO_2 is considered to be a milestone in the discovery of p-type TCO thin films, which has attracted widespread attention. Subsequently, various p-type films appeared, such as ZnO:N , NiO:Li , $\text{In}_2\text{O}_3:\text{Ag}_2\text{O}$ and so on. In 1997, Kawazoe et al. prepared CuAlO_2 thin films using pulsed laser deposition for the first time, with a conductivity of $9.5 \times 10^{-4} \text{ S/cm}$, a carrier concentration of $1.3 \times 10^{17} \text{ cm}^{-3}$, and a visible area transmittance in the range of 30–60%. Banerjee et al. reported a CuAlO_2 thin film prepared by DC sputtering with a conductivity of 0.08 S/cm and a transmittance of about 70% in the visible range. CuAlO_2 films have been prepared by various methods, including pulsed laser deposition, magnetron sputtering, chemical vapor deposition, hydrothermal methods, sol-gel methods, and spray pyrolysis. Although great progress has been made in p-type transparent conductive films, for the n-type transparent conductive films, the resistivity, mobility, stability, and repeatability of the experiments still require much work. There is a need for research into the conductive mechanism, synthetic technology, and potential application areas.

As a typical representative of nanomaterials, carbon nanotube (CNT) films exhibit good characteristics in terms of conductivity, light transmission, and flexibility, so they are of great interest to much scientific research. CNTs are used to synthesize transparent conductive films with wide permeable bands, stable mechanical properties, low costs, and other advantages. In 1997, the research group of Jiesi Shen, at the Institute of Physics, Chinese Academy of Sciences, through catalytic chemical vapor deposition technology directly achieved high conductivity and high transparency CNT film, achieving growth of a transparent film in a $5 \text{ cm} \times 10 \text{ cm}$ area with an even film growth level. For a 100 nm thick film, the resistivity was up to $50 \text{ } \Omega \cdot \text{cm}$, with light transmittance of 70% or more. In 1997, the Márcio Dias Lima Study Group, at the Max-Planck Institute for Solid State Research in Germany, developed a new method of compressing the catalyst onto a specific area of the substrate by lithography, directly growing the CNT network. This method greatly improved the conductivity of the film, and significantly improved its light transmittance, increasing it to 94%. The main methods of preparing CNT film are divided into wet and dry methods.

The wet synthesis methods are typically carried out using homogeneous CNT dispersion solutions, including the vacuum filtration transfer method, spray coating method, spin coating method, pulling method, Langmuir–Blodgett (LB) method, electrophoresis and others. Dry synthesis methods include the aerosol direct synthetic method, the super array pull method and so on. Therefore, rapid and efficient preparation of a large area of flexible film is the main trend in the development of CNT transparent conductive film preparation.

Graphene has a special band structure, showing many peculiar properties. The results show that the electron transfer rate of graphene is as high as 8×10^5 m/s and the electron mobility at room temperature is 2.5×10^5 cm²/(V·s). Ideal monolayer graphene has only (2.3 ± 0.1) % opacity under white light and its reflectivity is negligible. Due to the high carrier mobility of graphene, it is the only alternative material for future transparent conductive films, which will be able to form high-transparent conductive materials that could transmit all infrared rays.

§1.3 Introduction to the Facing-Target DC-sputtering Technique

Over the course of recent years, the direct current (DC) and radio frequency (RF) sputtering techniques have been used extensively in two configurations, with a balanced or unbalanced magnetron. Their main applications have been in the fields of industry and research. Examples of industrial applications are: decorative thin films, hard wear-resistant thin films, low-friction thin films, corrosion-resistant thin films, thin films used as protective optical systems, and perhaps the most interesting application, thin films used in the electronic industry. In research, investigation has been oriented towards understanding the main physical mechanisms, such as interactions between charged particles and the surface of the target material, adherence between the substrate and the deposited material, and chemical reactions near the substrate, as well as the influence of the deposit parameters (substrate temperature, working pressure, power density applied to the target). This research has produced thin films with a high degree of crystallinity and with the possibility of various industrial applications.^[17]

Moreover, researchers have tried to improve the system of the sputtering technique. These efforts were initiated through the so-called “conventional” or balanced magnetron sputtering in the early 1970s, followed by the development of unbalanced systems in the late 1980s and incorporation into multi-source “closed-field” systems in the early 1990s. Recently, the sputtering technique has been able to increase the rate of deposition and ion energy by applying a unipolar high power pulse of low frequency and low duty cycle to the cathode target, referred to as high-power impulse magnetron sputtering or high-power pulsed magnetron sputtering. Common to all highly-ionized techniques is the use of very high-density plasma. Implementation of these discharges in sputter deposition technology modifies the surface of components, improving mechanical, chemical, optical, electronic, and other properties of the material. High-current glows are transient discharges operating at both high voltage ($> 300 \text{ V}$) and high current density ($> 100 \text{ mA cm}^{-2}$) simultaneously. They have recently proven successful for the deposition of thin-film materials. These developments have made possible an exceptionally versatile technique, suitable for the deposition of high-quality, well-adhered films of a wide range of materials with high rates of deposition. Table 1 gives the main applications obtained in the last decade with RF and DC magnetron sputtering.

Table 1 Technological applications of thin films obtained with magnetron sputtering

Technique	Coating
Balanced magnetron	Nano-composites of NC-TiC wear applications
Balanced magnetron	Optical properties of AlSiN nano-composites
Balanced magnetron	Hard coatings to decorative applications
Balanced magnetron	Nd-Fe-B Film for magnetic applications
Balanced magnetron	Optical applications.
Unbalanced magnetron	Hard films for corrosion and wear applications
Unbalanced magnetron	Nb Films for biological applications
Unbalanced magnetron	NbO films for biological applications
Unbalanced magnetron	Electrical applications of NbN films.
Unbalanced magnetron	Diamond-like carbon films for infrared transmission enhancement
High power pulsed magnetron sputtering	Thin films for automotive engineering
High power pulsed magnetron sputtering	TiAlCN/VCN films for tribological applications

In sputtering, there are two means of operation: DC and RF, which also function in two configurations: magnetron DC and magnetron RF. In DC discharge, the cathode electrode is the sputtering target and the substrate is placed on the anode, which is often at ground potential. The applied potential appears across a region very near the cathode, and the plasma generation region is near the cathode surface. The cathode in DC discharge must be an electrical conductor, because an insulating surface develops a surface charge that prevents ion bombardment of the surface. This condition implies that DC sputtering must be used to sputter simple electrically conductive materials such as metals, although this process is slow and expensive

compared to vacuum deposition. An advantage of DC sputtering is that the plasma can be established uniformly over a large area, so that a solid large-area vaporization source can be established.

However, in DC sputtering the electrons that are ejected from the cathode are accelerated away from the cathode and are not used efficiently to sustain the discharge. To avoid this effect, a magnetic field is added to the DC sputtering system that can deflect the electrons to near the target surface, and with appropriate arrangement of the magnets, the electrons can be made to circulate on a closed path on the target surface. This high current of electrons creates high-density plasma, from which ions can be extracted to sputter the target material, producing a magnetron sputter configuration. A disadvantage of the magnetron sputtering configuration is that the plasma is confined near the cathode and is not available for activation of reactive gases in the plasma near the substrate for reactive sputter deposition. This difficulty can be overcome by using an unbalanced magnetron configuration, where the magnetic field is such that some electrons can escape from the cathode region. A disadvantage of the unbalanced magnetron is that the current of escaping electrons is not uniform; hence the plasma generated is not uniform.

Prof. Moriga's research team in Tokushima University has worked for many years on developing the preparation of transparent conductive films using a facing-target DC-sputtering technique and designed the DC sputtering apparatus shown in Fig.1. ^[18] The substrate holder can be heated up to 400 °C and it can be rotated at speeds up to 60 rpm. This is useful and convenient for control of the composition of thin film, to attain its homogeneity.

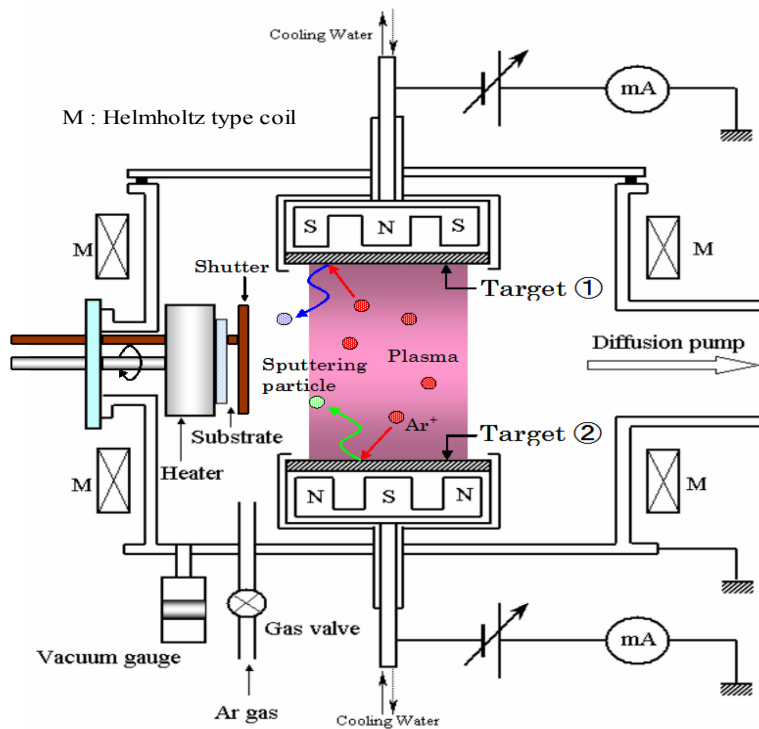


Fig.1 Direct current magnetron sputtering

§1.4 Research Topics and Contents

At present, the most widely used transparent conductive film materials are tin oxide-based on ITO and FTO. ITO has been used in the front electrode of photovoltaic cells. However, to meet the optical absorption performance requirements, TCO glass must have the ability to improve light scattering, and ITO coating can obstruct this. Indium is a rare element, its content in the crust is 5–10%, and it is not present in independent mineral form; however, it is widely distributed in sphalerite, and therefore, it is expensive. ITO used in solar cells is not stable in plasma, has a small substrate size, is toxic, and its laser etching performance is also poor. Hence, the current use of ITO coating has been in non-photovoltaic cell mainstream electrode glass. FTO glasses, because of electrochromic and photocatalytic aspects of its light transmittance and conductivity have a high demand in dye-sensitized solar cells. For optical applications, good transmittance of visible light and good reflectivity of infrared are required. The basic requirements are: low surface resistance, high

transmittance, large area, light weight, easy processing, and impact resistance. FTO is used primarily in the production of glass for construction. Its conductivity is slightly worse than that of ITO, but it has a relatively low cost, and easy laser etching.

At present, China has only been able to develop transparent conductive film with an average visible light transmittance of about 80%, and has not been able to achieve transmittance of more than 90%. In the field of high transmittance, low resistance transparent conductive film research, both opportunity and challenge coexist, and more in-depth study is required.

In this doctoral dissertation, we selected the new material In-Ga-Zn-O (IGZO) oxide as the research subject, and explored its experimental preparation method. The material composition, effects on size, material structure, surface morphology, optical effects, electrical characteristics, and practical experimental basis were investigated.

After a large amount of basic experimental research, scientists have turned to the use of computer simulation tools to understand the microstructure of materials and relevant material properties and hence to study the effects of material composition on performance improvement. This is particularly useful in the field of semiconductor materials, to study the doping of atomic species, the concentration of the semiconductor band material, the nature of electronic transport properties, and the magnetic, and other, behavior changes. To explain the differences in material properties caused by transformation on a microscopic scale of the material, the author uses the first-principles method to construct the appropriate crystal parameters; optimize the unit cell structure; and obtain the density, energy structure of the material, density distribution of electrons, analysis of atomic position and charge distribution, and so on. Based on this, the relationship between the microstructure and the properties of the material has been analyzed rationally.

Chapter 2: Processes of Transparent Conductive Oxides

§2.1 Raw Materials

For the preparation of a-IGZO thin films, an insulative Ga₂O₃ target cannot be used in DC magnetron sputtering. However, it is obvious that the use of IZO and GZO combination targets will result in a shortage of Ga content in the deposited thin films.

Ga₂O₃ pellets with a disk shape ($\phi=10$ mm, 0.5 g in weight) were placed geometrically in the erosion region on the IZO target to enrich the Ga content of the films. The number of Ga₂O₃ pellets was defined as n. For the ITZO, ZnO, and ITO targets (manufactured by Mitsui Mining & Smelting Co., Ltd, with a ratio of 90:10 In₂O₃/SnO₂ for ITO) were used for film deposition

§2.2 Experimental Instruments for Direct Current Magnetron Sputtering (DCMS)

According to the sputtering source used, magnetron sputtering has both DC and RF points. The main difference between the two is the way the gas is discharged. For the simplest DC sputtering, the target is the cathode, the substrate and its fixed frame are the anode, ionized argon ions in the electric field accelerate bombardment of the target, and the sputtering target atoms are deposited on the substrate surface, and grow into a thin film. The DC sputtering operation is simple, and three parameters (pressure, sputtering voltage, sputtering current) can be controlled. However, its low sputtering rate, high substrate temperature, and other shortcomings significantly constrain its application, and the process is of little significance for industrial production.

For DC magnetron sputtering, the sputtering target is set in a specific magnetic field source so that the magnetic field direction of the target surface is perpendicular to the direction of the electric field. The electrons have trajectories similar to wheel trajectories on the surface of the target, increasing their chances of collision with Ar, and hence improving the sputtering efficiency. Compared with simple DC sputtering, the magnetron sputtering deposition rate is high, substrate temperature is low, and damage to the film is small.

Based on the experimental requirements, the DC magnetron sputtering technique was used in this research.

§2.3 Experimental Processes

The principle of magnetron sputtering is that the electrons collide with the argon atoms in the process of flying to the substrate under the action of the electric field E , and the ionization produces Ar^+ ions and new electrons. These new electrons fly to the substrate, and the Ar^+ ions in the electric field accelerate their flight to the cathode target, so there is high energy bombardment of the target surface, leading to target sputtering. By this sputtering of particles, neutral target atoms or molecules are deposited on the substrate to form a thin film, and the resulting secondary electrons are affected by the electric field and magnetic field, B , resulting in a direction of $E \times B$ refers. This drift, referred to as $E \times B$ drift, has a movement trajectory similar to that of a cycloid. If the magnetic field is a ring, it causes the electrons in cycloid-form in the target surface to have a circular motion; they cover a large area and are bound to a plasma region near the target surface; therefore, a large amount of Ar is ionized in the region to bombard the target, thereby achieving high deposition rate. As the number of collisions increase, the energy of the secondary electrons is depleted, they gradually move away from the target surface, and are eventually deposited on the substrate under the action of the electric field E . Because of the low energy of these electrons, the energy delivered to the substrate is small, resulting in a lower substrate temperature rise. Magnetron sputtering is the collision process between the incident particles and the target. Incident particles collide with the target through a complex scattering process, and during this collision with target atoms, part of their momentum is transmitted to the target atoms. The target atoms then collide with other target atoms, leading to a cascade process. The target atoms near some of the surfaces of the cascade are given sufficient momentum to move outward and are sputtered away from the target.

§2.4 Material Characterization

X-ray diffraction analyses were conducted (Rigaku, RINT2500 VHF) with monochromatized $\text{Cu K}\alpha$ radiation to gain structural information about each film.

Surface morphology was examined using a scanning probe microscope (Seiko Instruments Inc. Nanopics 2100). Composition of the films was determined by X-ray fluorescent spectroscopy (Shimadzu Rayny EDX-800). The electrical properties, resistivity, Hall mobility, and carrier concentration of the films were determined using the Van der Pauw method via Hall-effect measurements (ECOPIA HMS-2000). The optical transmittance of the film was measured by a UV-Vis spectrometer (JASCO V-670), and the film thickness was estimated from the optical interference observed between the film and substrate.

The performance requirements for transparent conductive oxide films depend on whether they are being used for active or passive effects in the device. For the active role, detailed electrical and optical parameters of the transparent conductive oxide film itself, and the crystallinity, defects, etc. must be known, and there are more stringent requirements. In the passive case (usually used as a transparent electrode), the transparent conductive oxide semiconductor film is required only to have a low block resistance and a high visible light transmittance, with no special requirements for other electrical and optical applications. However, since the block resistance and the transmittance both increase with the thickness of the transparent conductive oxide film, it is not possible for the same transparent conductive film to satisfy both the best block resistance and the best light transmittance; a trade-off method must therefore be used. Once the two parameters are selected, it is useful to quickly evaluate and compare the performance of the transparent conductive oxide film.

Chapter 3: Experimental Research on In-Ga-Zn-O Materials

§3.1 In-Ga-Zn-O thin films by DC magnetic sputtering.

Amorphous In-Ga-Zn-O (a-IGZO) thin films were deposited on glass substrates by DC co-sputtering of IZO ($\text{In}_2\text{O}_3/\text{ZnO}$ ratio of 90:10, manufactured by Idemitsu Kosan Co., Ltd) and GZO (12.5 wt% Ga, manufactured by Mitsui Mining & Smelting Co., Ltd) targets. Currents (current ratio: $\delta = I_{\text{GZO}} / (I_{\text{GZO}} + I_{\text{IZO}})$) applied to the targets were controlled independently, with the sum of the currents fixed at 60 mA. Deposition was carried out at room temperature at an argon gas base-pressure of 1.3×10^{-1} Pa. Ga_2O_3 pellets with a disk shape ($\phi = 10$ mm, 0.5 g in weight) were placed geometrically in the erosion region on the IZO target to enrich the Ga content of the films. The number of the Ga_2O_3 pellets was defined as n .

For this research, the experimental parameters refer to literature from the Moriga research team in Tokushima University.^[18, 21, 22]

§3.2. Material Characterization

X-ray diffraction analyses were conducted (Rigaku, RINT 2500 VHF) with monochromatized Cu $K\alpha$ radiation to gain structural information about each film. Surface morphology was examined using a scanning probe microscope (Seiko Instruments Inc. Nanopics 2100). Composition of the films was determined by X-ray fluorescent spectroscopy (Shimadzu Rayny EDX-800). The electrical properties, resistivity, Hall mobility, and carrier concentration of the films were determined using the Van der Pauw method via Hall-effect measurements (ECOPIA HMS-2000). The optical transmittance of the film was measured by a UV-Vis spectrometer (JASCO V-670), and the film thickness was estimated from the optical interference observed between the film and substrate.

In our previous work, we demonstrated that relatively low resistivity could be obtained for IZO deposited at an argon pressure of 1.3×10^{-1} Pa; therefore, this pressure was applied for all depositions in this work.

Figure 2 shows the variation in electrical properties of IGZO films deposited on glass at different current ratios (δ). When δ was increased, the Hall mobility of the IGZO film decreased, its carrier concentration decreased, and its resistivity increased. It is generally considered that the number of free carriers, important for electrical conduction, decreases with an increase in the amount of ZnO, and oxygen vacancies decrease with an increasing amount of Ga, with inhibition of the generation-free carriers.

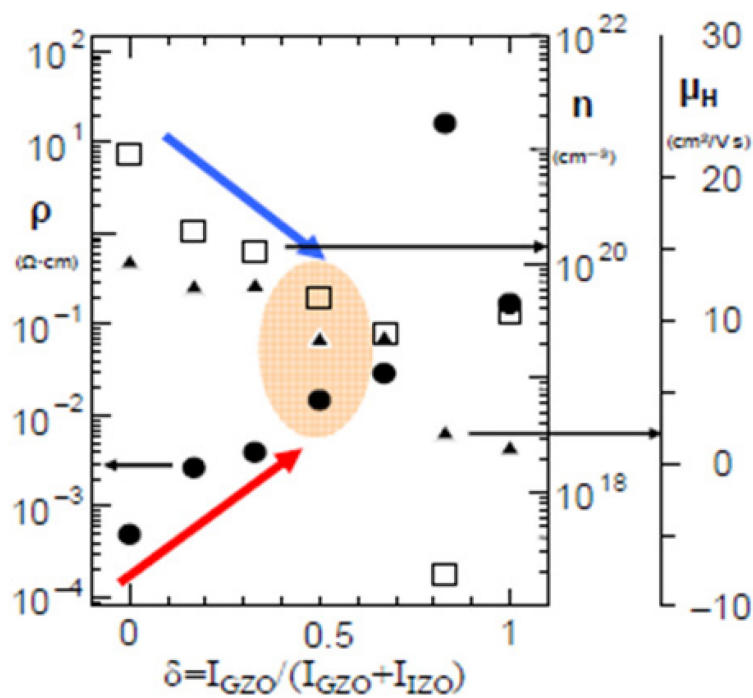


Fig. 2. Electrical properties, ● resistivity ρ , □ carrier concentration n , and ▲ Hall mobility μ_H , of IGZO films deposited at various δ values.

Figure 3 shows the metal composition of IGZO films deposited at various δ values. The semiconductor layer of TFT is required to have a high Hall mobility and high resistivity, so $\delta=0.5$ was thought to be the most suitable value. The thin film at $\delta=0.5$ was found to have a composition of In/Ga/Zn=61:3:36, implying that the ratio of (In+Ga) to Zn was 2:1, corresponding to the ideal composition of bulk IGZO, InGaZnO_4 .

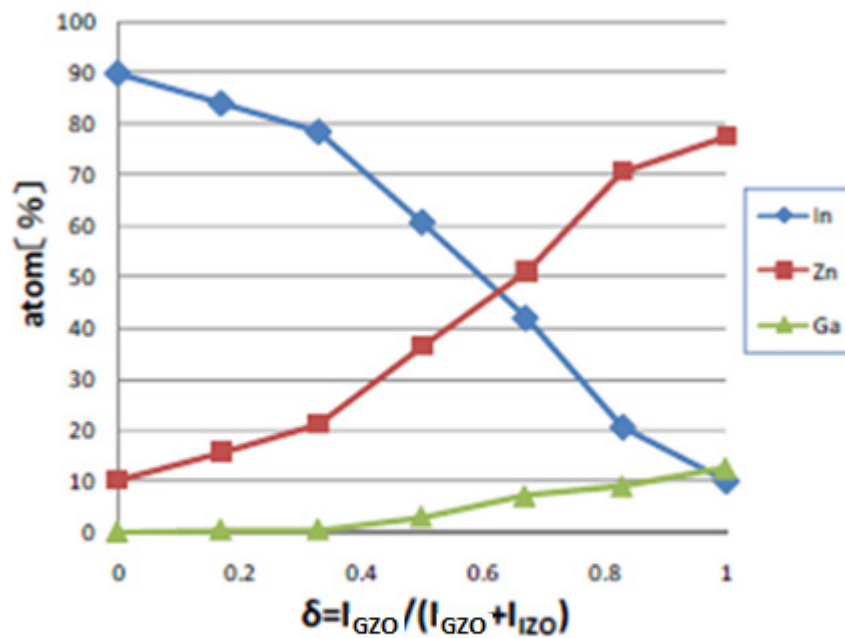


Fig. 3. Metal composition ratios of IGZO films deposited at various δ values.

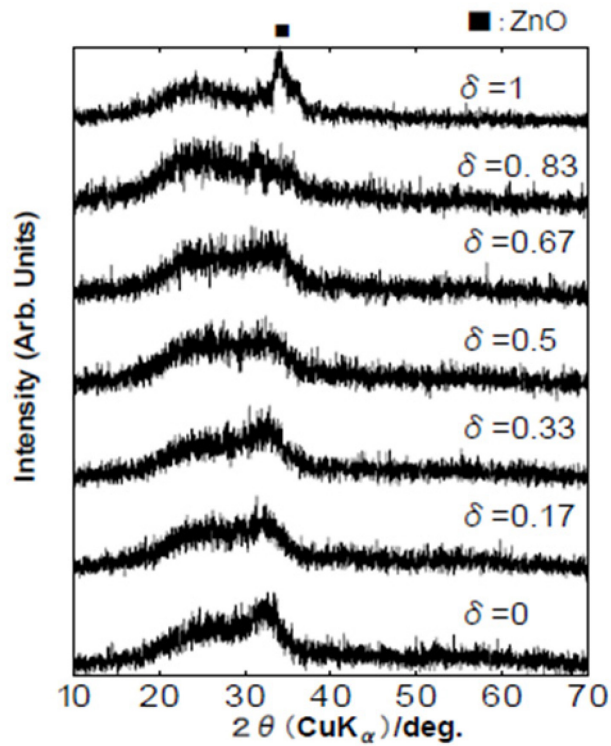


Fig.4. XRD patterns for IGZO films deposited at various δ values.

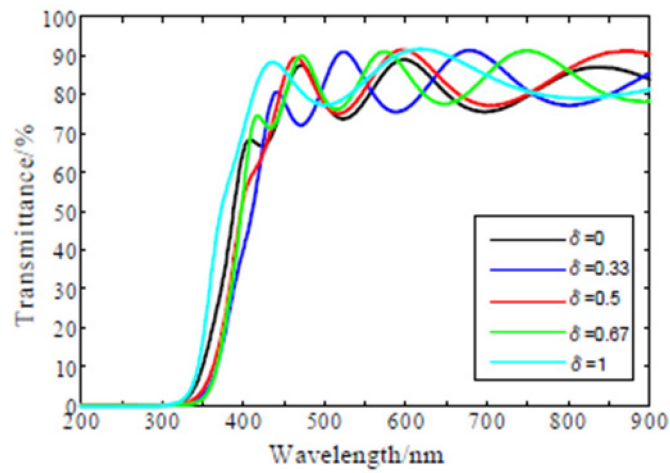


Fig.5. Optical transmission spectra for IGZO films deposited at various δ values.

Figure 4 shows X-ray diffraction patterns for IGZO thin films deposited on the glass substrates as a function of current ratio. An amorphous phase was observed and was in the δ ($\delta = I_{GZO}/(I_{GZO}+I_{IZO})$) range from 0 to 0.83. The thin film

deposited at $\delta=1$ contained a contribution from preferentially oriented wurtzite-type ZnO, shown by the appearance of a weak ZnO (002) peak.

Figure 5 shows optical transmission spectra for IGZO films deposited at various δ values. The average transmittance of each film in the visible region (380–760 nm) was greater than 77%.

Figure 6 shows atomic force microscopy (AFM) images for IGZO films deposited at various δ values. The surface roughness of the films was quantified by the average roughness (Ra). Figure 6 also shows the Ra values for the IGZO films deposited at different δ values. The Ra values increased as δ values increased up to 1.15 nm. We found that the surface uniformity of all films was improved by the introduction of Zn atoms. The film at $\delta=1$ possessed increased surface roughness, because of the strong c-axis orientation and preferential growth of ZnO as observed by XRD.

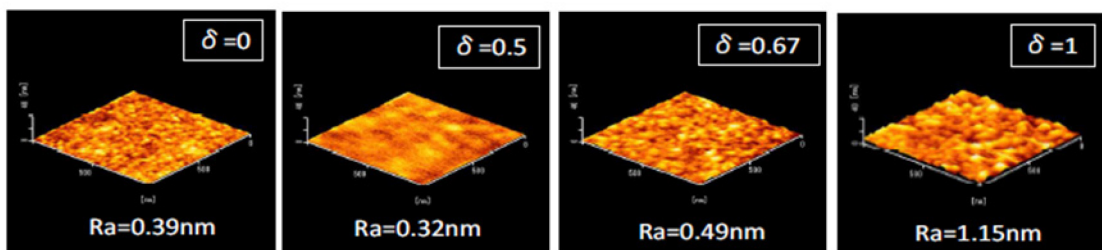


Fig. 6. AFM images for IGZO films deposited at various δ values.

As seen in Figure 3, the Ga content in the IGZO films was too small to be compared with the ideal IGZO composition, InGaZnO_4 .

Figures 7 and 8 show the composition and electrical properties of IGZO films deposited using an ITO target on which a specified number of the Ga_2O_3 pellets were placed to enrich the gallium content. At a δ value of 0.5, the Ga content increased with an increasing number of Ga_2O_3 pellets. As a result, with increasing n , the film composition approached a ratio of 1:1:1 of In/Ga/Zn. The electrical properties of the a-IGZO films as a function of n revealed that increasing the Ga content resulted in

increased electrical resistivity and a decreased carrier concentration. The increased electrical resistivity suggests that the formation of free carriers was inhibited by the highly covalent Ga-O bond. The Hall mobility of the a-IGZO films remained unchanged.

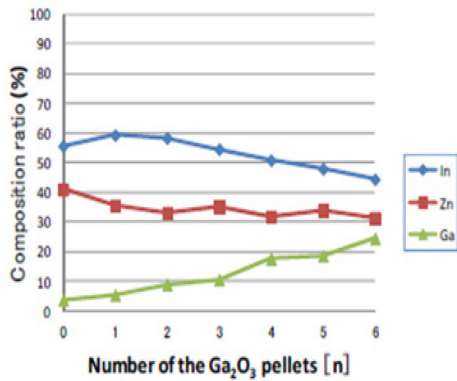


Fig. 7. Composition of Ga-enriched IGZO films deposited with various number of pellets (n).

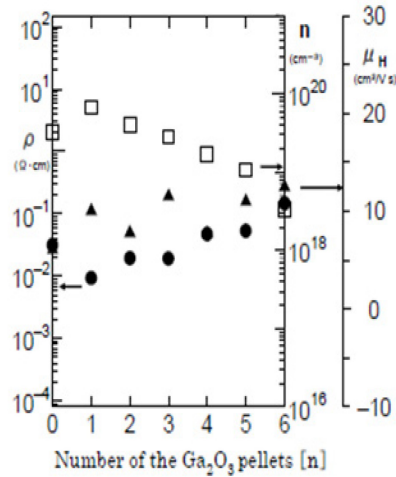


Fig. 8. Electrical property, ● resistivity ρ , □ carrier concentration n , and ▲ Hall mobility μ_H , of Ga-enriched IGZO films deposited with various number of the pellets (n).

§3.3. Brief Summary

In the present study, excellent electrical properties were obtained for IGZO thin films in the semiconductor layer of TFTs. The Hall mobility of the composition-optimized thin film reached to 12 cm²/(V·s), with a resistivity of 0.15 Ω · cm. The Hall mobility attained is ten times larger than that of amorphous silicon (a-Si, reference), and is the same as that of a commercial IGZO thin film. The composition obtained was In/Ga/Zn in the ratio of 1:1:1, which is the ideal IGZO composition, InGaZnO₄.

Chapter 4: Experimental Research on In-Sn-Zn-O Material

§4.1. In-Sn-Zn-O thin films by DC magnetic sputtering

For ITZO, ZnO and ITO targets (manufactured by Mitsui Mining & Smelting Co., Ltd, In₂O₃/SnO₂ in the ratio of 90:10 for ITO) were used for film deposition. The experimental conditions for the deposition were the same as that for IGZO. The current ratio was defined as $\delta = I_{\text{ZnO}} / (I_{\text{ZnO}} + I_{\text{ITO}})$.

§4.2. Material Characterization

X-ray diffraction analyses were conducted (Rigaku, RINT 2500 VHF) with monochromatized Cu K α radiation to gain structural information about each film. Surface morphology was examined using a scanning probe microscope (Seiko Instruments Inc. Nanopics 2100). Composition of the films was determined by X-ray fluorescent spectroscopy (Shimadzu Rayny EDX-800). The electrical properties, resistivity, Hall mobility, and carrier concentration of the films were determined using the Van der Pauw method via Hall-effect measurements (ECOPIA HMS-2000). The optical transmittance of the film was measured by a UV-Vis spectrometer (JASCO V-670), and the film thickness was estimated from the optical interference observed between the film and substrate.

In previous research, we demonstrated that relatively low resistivity could be obtained for IZO deposited at an argon pressure of 1.3×10^{-1} Pa, therefore, this pressure was applied for all depositions in this work. Many researchers have investigated these new oxide semiconductor materials. ^[23, 24]

Figure 9 shows the variation in the electrical properties of ITZO films deposited at various δ values. When the current ratio δ was increased, the carrier concentration and mobility of ITZO films decreased, and the resistivity increased. It was found that the free carriers, responsible for electrical conduction, decreased with an increasing amount of ZnO. The resistivity of the ZnO-ITO films was higher than that of the Sn-free IZO films. It is suggested that Sn-O bond is more covalent than those of In-O and Zn-O, inhibiting the formation of oxygen vacancy-generated free carriers.

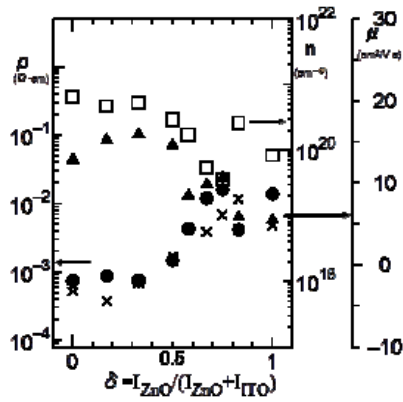


Fig. 9. Electrical properties, ● resistivity ρ (circles for ITZO and crosses for Sn-free IZO for reference), □ carrier concentration n , and ▲ Hall mobility μ , of ITZO films deposited at various δ values.

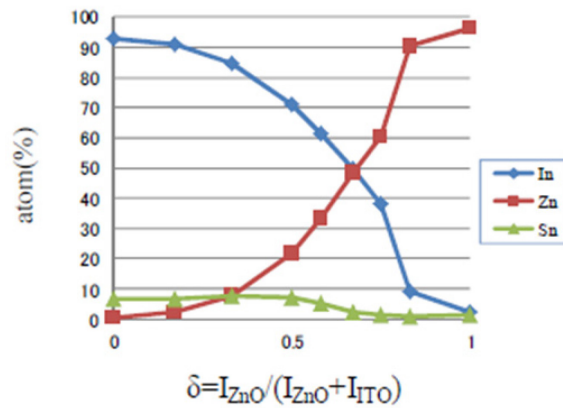


Fig. 10. Metal composition ratios of ITZO films deposited at various δ values.

Figure 10 shows the compositions of ITZO films deposited at various δ values. The semiconductor layer of TFTs requires a high Hall mobility as well as high resistivity; the film deposited at $\delta=0.75$ displayed the best characteristics. The thin film at $\delta=0.75$ possessed a composition of Zn/In/Sn in the ratio of 60:38:2, which contained excess zinc compared to other ITZO films reported.

Figure 11 shows X-ray diffraction patterns for ITZO thin films deposited on glass substrates as a function of current ratio. The δ -range in which the amorphous

phase was observed was from 0–0.83. The thin film deposited at $\delta=1$ possessed preferentially oriented wurtzite-type ZnO crystal shown by the enhanced characterized (002) peak. As the film consisted of ZnO without dopants, it appeared that the crystallinity of the ZnO thin film at $\delta=1$ was significantly higher than that of the GZO film prepared at $\delta=1$, depicted in Figure 4.

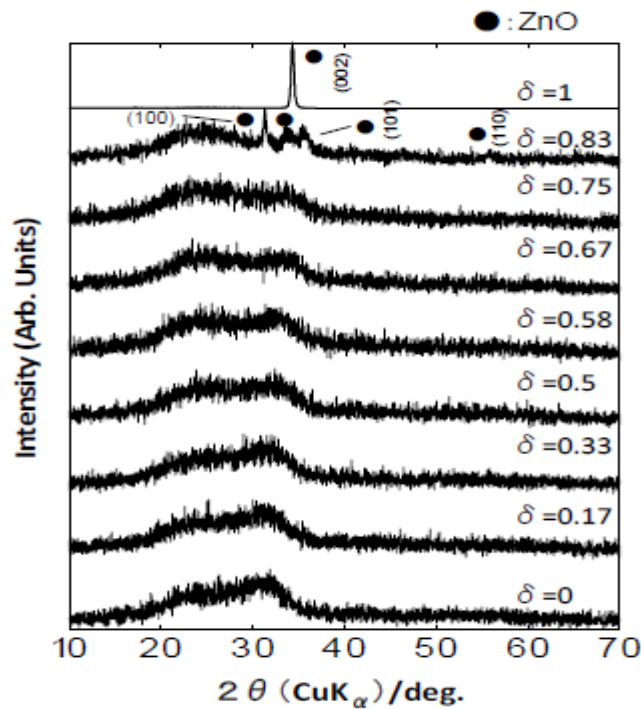


Fig. 11. XRD patterns for ITZO films deposited at various δ values.

Figure 12 shows optical transmission spectra for ITZO films deposited at various δ values. The average transmittance of each film in the visible region (380–760 nm) was greater than 75%. The transmittance of ITZO films is comparable to that of the IGZO films. As can be seen in Figure 12, the transmittance of the ITZO films was higher than that of the ITO film at $\delta = 0$, probably due to the contribution of ZnO, which usually yields high transmittance films.

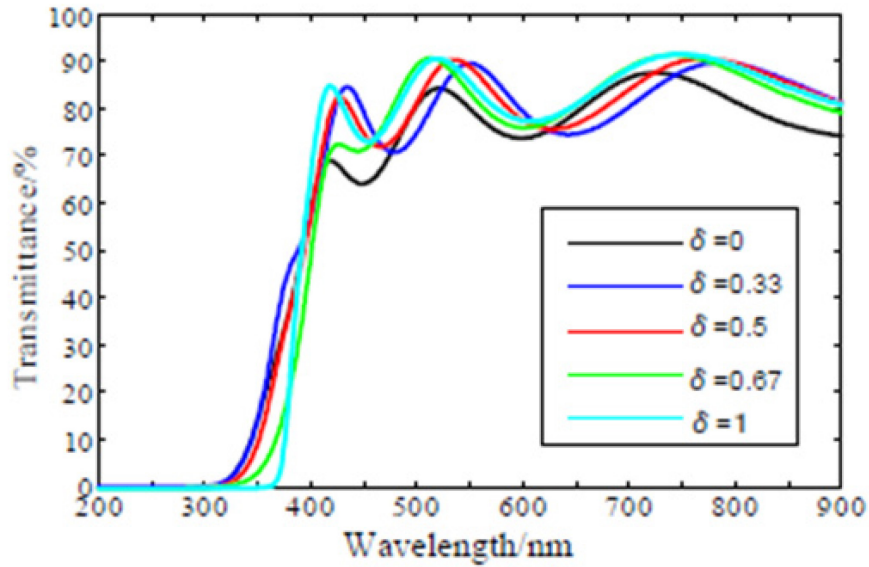


Fig.12. Optical transmission spectra for ITZO films deposited at various δ values.

Figure 13 shows AFM images of ITZO films deposited at various δ values. The average roughness (Ra) of ITZO films increased up to 1.49 nm as δ increased. The thin film at $\delta=1$ possessed increased surface roughness, because of the strong c-axis orientation and preferential growth of ZnO, as observed by XRD.

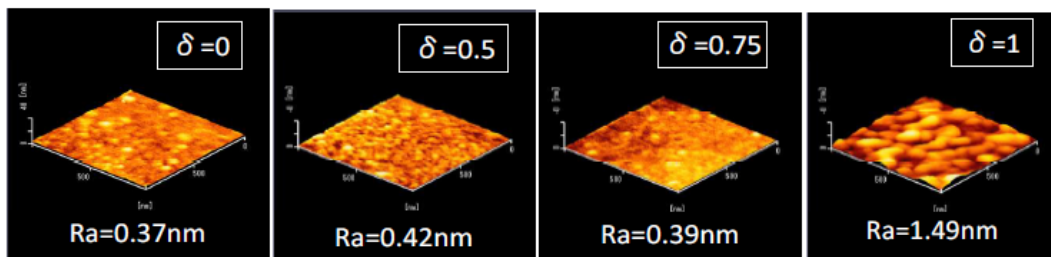


Fig.13. AFM images of ITZO films deposited at various δ values.

The tin content in the ITZO films was low; suggesting that optimization of the tin content could be needed. Figure 14 shows the electrical properties of ITZO films deposited using an ITO target on which a designated number n of the SnO_2 pellets were put to enrich the tin content. The current ratio was 0.75 ($\delta = I_{\text{ZnO}} / (I_{\text{ZnO}} + I_{\text{ITO}})$) for all samples. Investigation of the electrical properties of a-ITZO films as a function of n revealed that the electrical resistivity showed a maximum value of $0.17 \Omega \cdot \text{cm}$ with a relatively high mobility of $10 \text{ cm}^2/(\text{V}\cdot\text{s})$ when sheets of SnO_2 pellets were added to the target. These values are almost compatible with those observed in the Ga-enriched IGZO films reported previously. The optimal composition of the IGZO film is Zn/In/Sn in a ratio of 62:31:7. This optimal composition showed high resistivity and mobility, and is currently being investigated further.

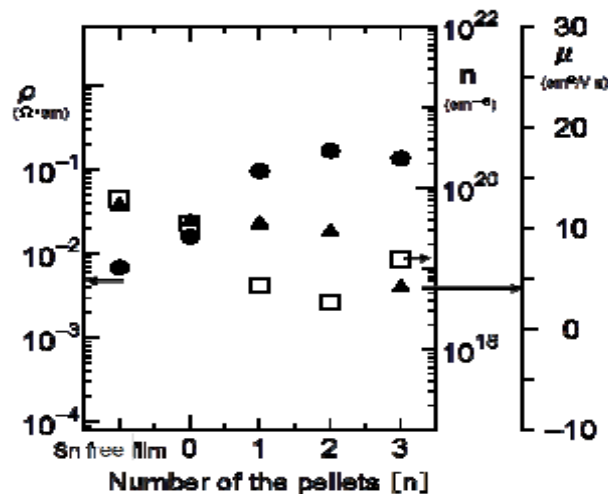


Fig. 14 Electrical properties, ● resistivity ρ , □ carrier concentration n , and ▲ Hall mobility μ , of Sn-enriched ITZO films deposited at various number of the pellets (n).

§ 4.3. Brief Summary

Amorphous ITZO films were obtained with electrical parameters of high resistivity ($0.17 \Omega \cdot \text{cm}$) and high mobility ($10 \text{ cm}^2/(\text{V}\cdot\text{s})$). The resistivity and mobility of the ITZO thin films were compatible with the IGZO thin films seen in this work, although the optimization of film composition is yet to be completed.

Chapter 5: Conclusions and future works

§5.1. Summary and Conclusions

New transparent conducting oxide (TCO) materials, indium-gallium-zinc-oxide (IGZO) and indium-tin-zinc-oxide (ITZO), were deposited on glass substrate by DC co-sputtering using IZO-GZO and IZO-ITO target combinations, respectively. Amorphous indium-gallium-zinc-oxide (a-IGZO) films possessing electron motilities of as high as $12 \text{ cm}^2/(\text{V}\cdot\text{s})$ and resistivity of $0.15 \Omega \cdot \text{cm}$ were deposited. The Hall mobility was ten times higher than that of amorphous silicon (a-Si), and comparable to that of commercial IGZO thin films.

A good electrical resistivity of $0.17 \Omega \cdot \text{cm}$ with a relatively high mobility of $10 \text{ cm}^2/(\text{V}\cdot\text{s})$ was found for the ITZO films. These values were similar to those observed for the IGZO films in this study.

§5.2. Suggestions for future works

1. Further optimize the experimental conditions for the TCO
2. Find other materials with properties able to decrease the resistance and increase the transmittances.

References:

- [1] David S.Ginley, Handbook of Transparent Conductors, Springer, 2010.
- [2] R. Ramprasad. First principles study of oxygen vacancy defects in tantalum pentoxide. J. of Appl. Phys. 2003, 94(9): 5609
- [3] G. S. Chae: A Modified Transparent Conducting Oxide for Flat Panel Displays Only. Jpn. J. Appl. Phys. Part 1, 2001. 40(3A). 1282.
- [4] K. Nomura, A.Takagi, T. Kamiya. Amorphous Oxide Semiconductors for High-Performance Flexible Thin-Film Transistors. Jpn. J. of Appl. Phys. 2006, 45(5), 4303
- [5] Boyd W. Veal, S. K. Kim, Peter Zapo, et al. Interfacial control of oxygen vacancy doping and electrical conduction in thin film oxide hetero-structures, Nature Communications, 2016, 7:11892
- [6] László Korösi. ·SzilviaPapp. Szabolcs Beke. Highly transparent ITO thin films on photo sensitive glass: sol–gel synthesis, structure, morphology and optical properties. Appl.Phys.A, 2012, 107:385
- [7] H. Hosono. Transparent conducting materials: Flexibility with a metallic skin, Nature Chemistry. 2012, 4, 252
- [8] B. Thangaraju. Structural and electrical studies on highly conducting spray deposited fluorine and antimony doped SnO₂ thin films from SnCl₂ precursor. Thin Solid Films. 2002,402 (1-2):71
- [9] U.Ozgur, Ya.I.Alivov, C.Liu, *et al.* A comprehensive review of ZnO materials and devices. J. Appl. Phys.2005, 98, 041301
- [10] B.E.Sernelius, K.F.Berggren,Z.C.Jin, *et al* Band-gap tailoring of ZnO by means of heavy Al doping. Phys. Rev. B. 1988, 37, 10244
- [11] Y.Z. Tsai, N.F. Wang, C.L. Tsai, Fluorine-doped ZnO transparent conducting thin films prepared by radio frequency magnetron sputtering. Thin Solid Films.2010, 518(17), 4955

- [12] D. F Paraguay, L. W. Estrada, N, D. Acosta, et al. Growth, structure and optical characterization of high quality ZnO thin films obtained by spray pyrolysis, *Thin Solid Films*, 1999, 35(1,2):192
- [13] J.G.Lu, S.Fujita, T.Kawaharamura, et al. Carrier concentration dependence of band gap shift in n -type ZnO:Al films. *J. Appl. Phys.*2007, 101(8): 83705
- [14] A. Takagi, K. Nomura, H. Ohta, H. Yanagi, T. Kamiya, M. Hirano, H. Hosono: Growth of epitaxial ZnO thin films on lattice-matched buffer layer: Application of InGaO₃ (ZnO)₆ single-crystalline thin film, *Thin Solid Films*, 2005,486 , 38.
- [15]. K. Nomura, H. Ohta, A. Takagi, *et al.* Room-temperature fabrication of transparent flexible thin-film transistors using amorphous oxide semiconductors, 2004, *Nature*, 432, 488
- [16] T. Kamiya, K. Nomura, M. Hirano, and H. Hosono, Electronic structure of oxygen deficient amorphous oxide semiconductor a -InGaZnO_{4-x}: Optical analyses and first-principle calculations. *Phys. Stat. Solid. C*, 2008, 5(9), 3098
- [17] Alfonso Edgar, Olaya Jairo, Cubillos Gloria Thin film growth through puttering technique and its applications. *Crystallization Science and Technology*. 2011
- [18] T. Moriga, Y. Hayashi, K. Kondo, Y. Nishimura, K. Murai, I. Nakabayashi, H. Fukumoto, and K. Tominaga: Transparent conducting amorphous Zn-Sn-O films deposited by simultaneous dc sputtering. *J. Vac. Sci. Technol. A*, 2004, 22 1705.
- [19] G. Haacke. New figure of merit for transparent conductors, *J. Appl. Phys.* 1976, 47, 4086
- [20] Tauc, J., Grigorovici, R., Vacuum, A.: Optical properties and electronic structure of amorphous germanium. *Phys. Stat. Sol.* 1966, 15,627
- [21] T.Moriga, T.Okamoto, K. Hiruta, A. Fujiwara, I. Nakanayashi, K. Tominaga, Structures and Physical Properties of Films Deposited by Simultaneous DC Sputtering of ZnO and In₂O₃ or ITO Targets, *J. Solid State Chem.*, 2000,155, 312
- [22] T. Moriga, K. Shimomura, D. Takada, H. Suketa, K. Takita, K. Murai, K.Tominaga.

In₂O₃-ZnO transparent conductive oxide film deposition on polycarbonate substrates. Vacuum, 2009, 83 557

[23] C. A. Hoel, T. O. Mason, J.F. Gaillard, K. R. Poeppelmeier. Transparent Conducting Oxides in the ZnO-In₂O₃-SnO₂ System, Chemistry of Materials, 2010, 12(34):3569

[24] D. Y. Lee, J. R. Lee, G. H. Lee, P. K. Song, Study on In-Zn-Sn-O and In-Sn-Zn-O films deposited on PET substrate by magnetron co-sputtering system, Surf. Coat. Technol., 2008, 202, 5718

6. Appendix: Section of CASTEP calculations

6.1 Theoretical Basis of First-Principle Calculations

The *ab initio* method is well known for its precise control of the structure at the atomic level, and the included tools can accurately predict the structure. The intrinsic properties of many semiconductor materials, such as energy band, electron density, carrier diffusion concentration, electron transport barrier, etc., can now be calculated using the first principle method accurately. Fig. 6-1 is first principle methods. Over the past decades, there have been many examples of virtual material design and characterization combined with its experiments, which are significant for changing trial and error methods in traditional material designs, accelerating the pace of new materials. In this thesis, the author explains the structure of transparent conductive film caused by changes in the optical and electrical properties through the first principle of Material Studio software.

After a large number of experimental basic research, scientists in order to understand the microstructure of materials and material properties of relevance, the use of computer simulation tools to study the material composition on the performance improvement. Especially in the field of semiconductor materials, doping atomic species and concentration for the material of the semiconductor band and electron transport properties, magnetic and other behavior changes. In order to explain the difference of material properties caused by the transformation of the microscopic scale of the material, the author uses the first-principles method to construct the appropriate crystal parameters, optimize the unit cell structure, and obtain the density. The energy structure of the material, the distribution of electron density, the analysis of atomic location and charge distribution and other data, as a basis for a reasonable analysis of the microstructure and characteristics of the relationship between the material.

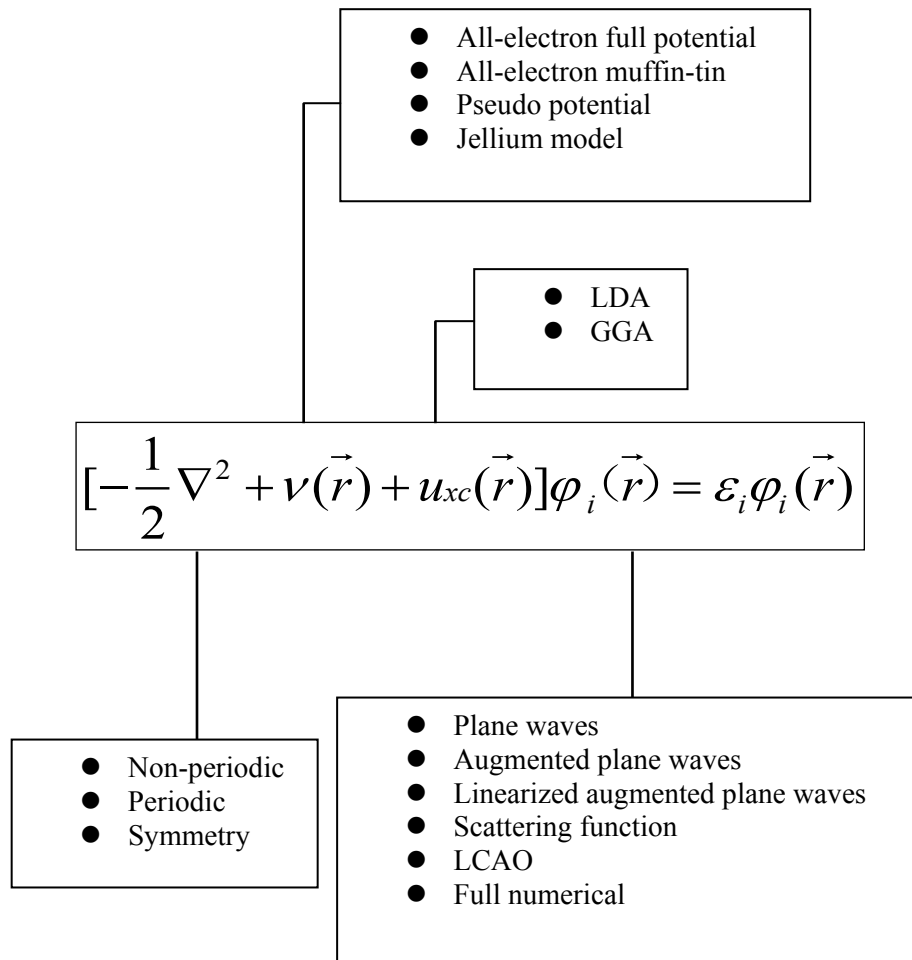


Fig.6-1. First Principle Methods

Since the electronic band structure is one of the most basic properties of the material, it has a profound effect on the practical application of the material. Therefore, the theoretical description of the electronic energy band structure has always been one of the most challenging problems in the first principle theory. The As a density functional theory for the theoretical calculation of the "standard model", there is a well-known "band gap problem" under the local density approximation or the generalized gradient approximation: the theoretical band gap of the semiconductor material has a significant system compared with the experimental value Sexual error.

The development of band theory is undoubtedly one of the most fundamental and far-reaching events in the field of modern condensed matter physics. Based on this concept, matter is divided into conductors, insulators and semiconductors. More importantly, the band theory provides a solid theoretical basis for describing the state of electron motion within a semiconductor material. It is this microelectronics level of understanding of the material, only half a century since the rapid development of microelectronics and information technology, which completely changed the basic face of human life.

As one of the most basic intrinsic properties of a material, the electronic band structure has a far-reaching influence on the applications in the fields of electronics, optics, optoelectronics and photo-catalysis. Therefore, the electron band structure has been the most theoretical principle One of the hot spots of concern. However, since the electronic band structure involves the electron excitation process, there are still many difficulties in its accurate and efficient theoretical treatment. Therefore, the first-principles theory of electronic band structure is still a very active and promising frontier field.

6.2 First-principles Calculation Simulation

6.2.1 Calculation Methods and Parameter Settings

Calculation method selection and parameter setting

The CASTEP module for Materials Studio allows you to set the parameters for a variety of requirements, with reasonable defaults that are sufficient for the common material research, but for challenging to new material properties, in order to publish the results in academic journals, and therefore to accept a more rigorous testing, it is still necessary to conduct a convergence test.

Common parameters that need to be subjected to the convergence test are: the quality of the system, the density of the plane wave, the density of the k-point sample, and the number of empty orbits (unoccupied) of the system when calculating the

optical properties. The empty track is used less, resulting in significant errors in the optical properties. Usually there is no need to change the artificial parameters, including self-consistent field energy tolerance for geometric optimization, atomic force and cell stress tolerance. The energy tolerance of the self-consistent field iteration is the difference between the total energy of the previous step and this step. The difference is less than the convergence threshold. The system automatically considers that the target has been reached and stops the self-consistent field iteration. As for the geometric optimization of the mechanical stress tolerance set, then affect the optimized crystal structure and the ideal minimum energy structure differences. In addition, the upper limit of the number of iterations of the band structure and the optical calculation may also need to be large when it encounters more complex crystals or more complex correlation calculations.

The CASTEP software is an ab initio quantum mechanics program based on the density functional theory (DFT). Based on the total energy plane wave pseudo potential theory, the atomic number and species prediction are used to include lattice parameters, structural properties, energy band structure, wave function, optical properties, Phonon spectrum, but only for the calculation of periodic structure. For strained materials obtained by epitaxial growth, on the one hand, the strained structure is cyclical due to the forced use of the crystal structure of the substrate; on the other hand, the lattice constant is different from that of the unstrained material due to stress. Therefore, CASTEP can be used to calculate the energy band of epitaxial growth strain material, and its lattice constant is the key to the construction of CASTEP calculation model.

In this thesis, the structure and optoelectronic properties of In-Ga-Zn-O material system are studied in the NF5220 computing server platform of INSPUR Co., Ltd., which is commercial first-principles calculation software. From the microstructure of the information to fully understand the material exhibited by the optical and electrical properties.

All calculations have been carried out using the density functional theory as implemented in CASTEP code. The norm conserving pseudopotentials (NCPPs) were employed to describe the Coulomb interactions between the valence electrons and

pseudo-ion core. The valence electrons were treated as: In: $5s^24d^{10}5p^1$, Ga: $4s^23d^{10}4p^1$, Zn: $4s^23d^{10}$, O: $2s^22p^4$ respectively. The kinetic energy cut-off value of 900 eV was used for plane wave expansion in reciprocal space. The sampling k-point mesh in the first irreducible Brillouin zone (BZ) was generated by Monkhorst-Pack method, using a $6 \times 6 \times 1$ grid for all studied structures. The lattice parameter and atomic positions were fully relaxed, and other convergence criteria were: 10^{-8} eV/atom in energy and 1×10^{-6} eV/Å in atomic force. The exchange-correlation density functional was treated within Perdew-Burke-Ernzerhof (PBE) of generalized gradient approximation (GGA). The quality of the q factor spacing was set to 0.01 \AA^{-1} , and the BZ path was set as Z-A-M-G-X-G-Z-R in this work. For electronic band structure and optical dielectric properties, we employed the range-separated hybrid density functional Heyd-Scuseria-Ernzerhof (HSE06). HSE06 has been shown to predict more reliable electron band structure and optical properties in many previous works.

6.2.2 Energy Band Analysis

The band gap of $\text{InGaZn}_2\text{O}_5$ is as show in Fig.6-2. Although it has direct gap, the gap is 3.1eV (The calculated value is very close to the experimental value form UV-VIS in chapter 2), between the X-points, while the latter's gap is from X_C to X_V . The conduction-band minimum (CBM) and the valence-band maximum (VBM) is at X point. The conduction-band is very steep peak at X-point, but the valence-band is very smooth peak at X-point.

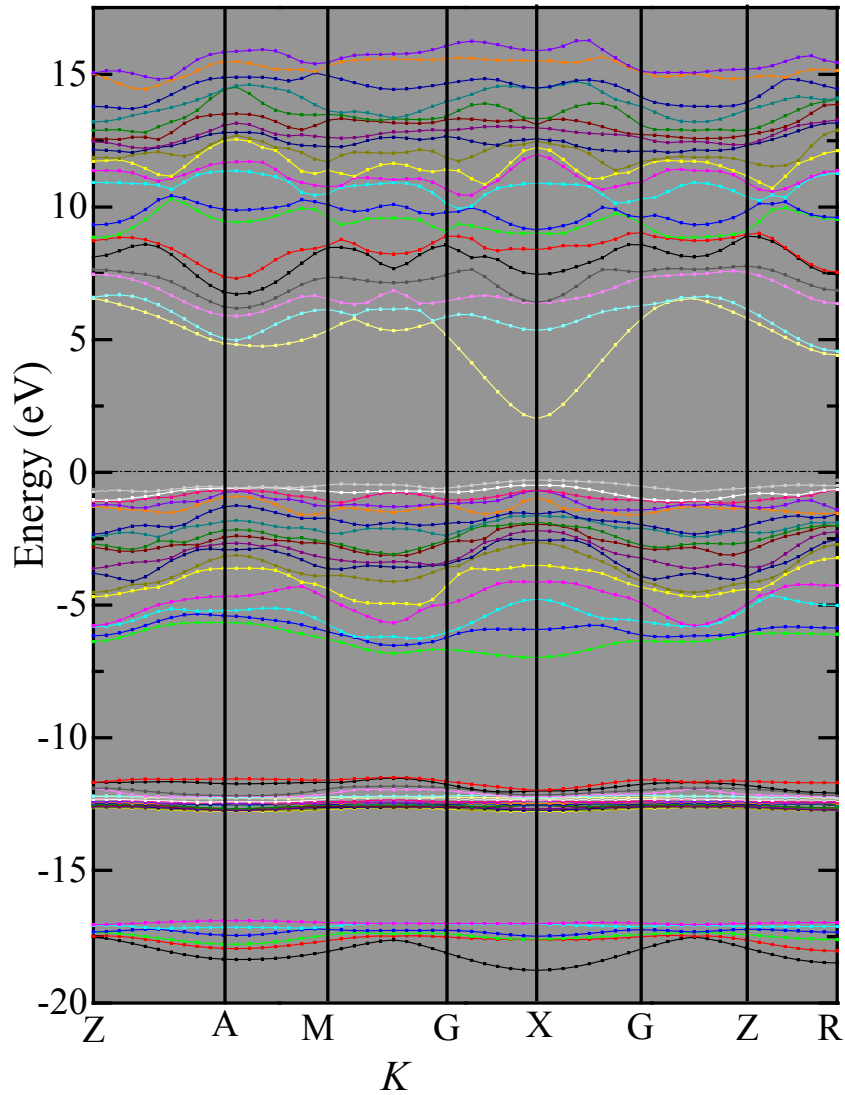


Fig.6-2. Band gap of InGaZn₂O₅

6.2.3 Density of States (DOS)

The total and partial densities of states (PDOS) of InGaZn₂O₅ have been calculated, as shown in Fig.6-3.and Fig. 6-4.respectively, atomic bonding characteristics are clearly illustrated in these PDOS at the Fermi energy. The Fermi level is set at $E = 0$ and it can be clearly seen that there is a certain value of Fermi energy (E_f) of total DOS at the Fermi level. Therefore, the compound in this work exhibit semi-conductivity. According to the results of other author it can be learnt that

the minimum (maximum) of the DOS qualitatively indicates compound stability (instability). Fig. 6-3 show is that the valence-band is spitted many sub band; the conduction-band is only one peak.

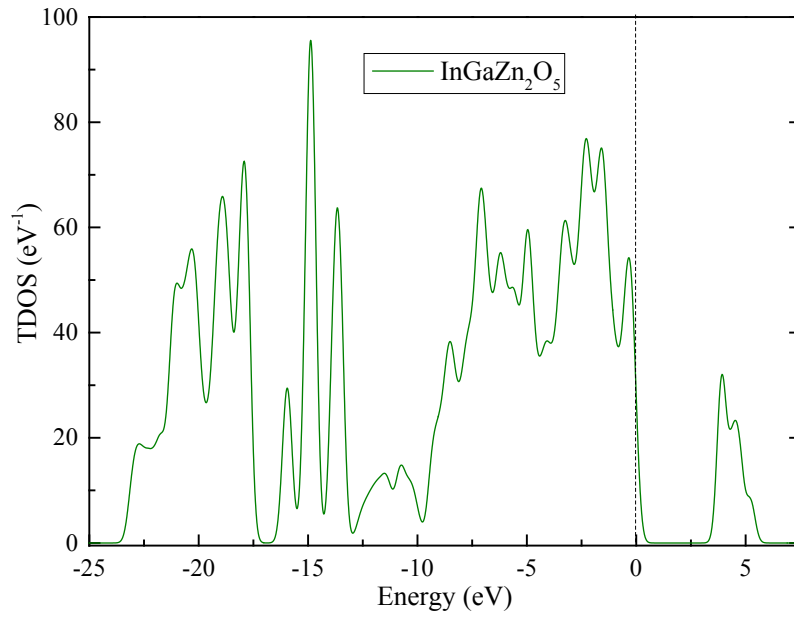
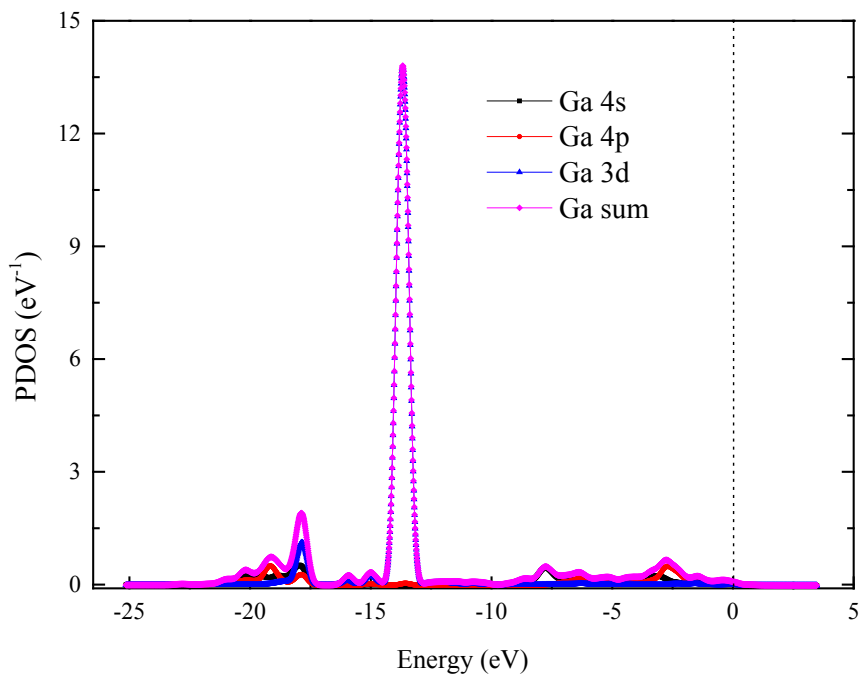
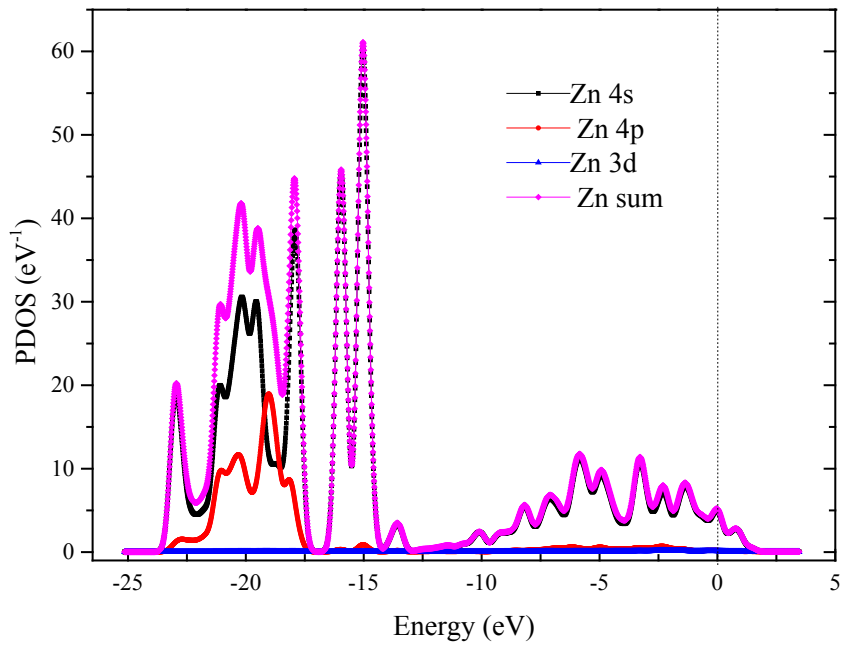
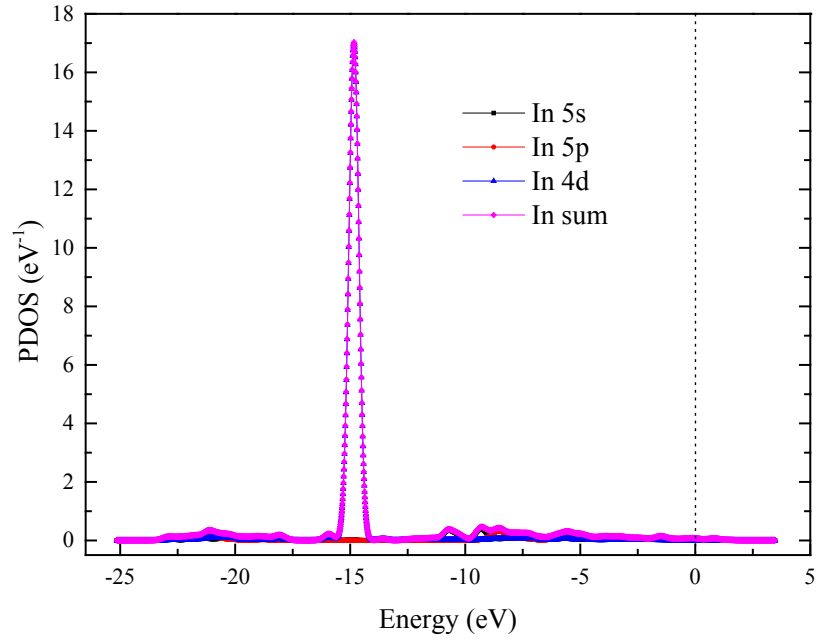


Fig 6-3. TDOS of InGaZn₂O₅





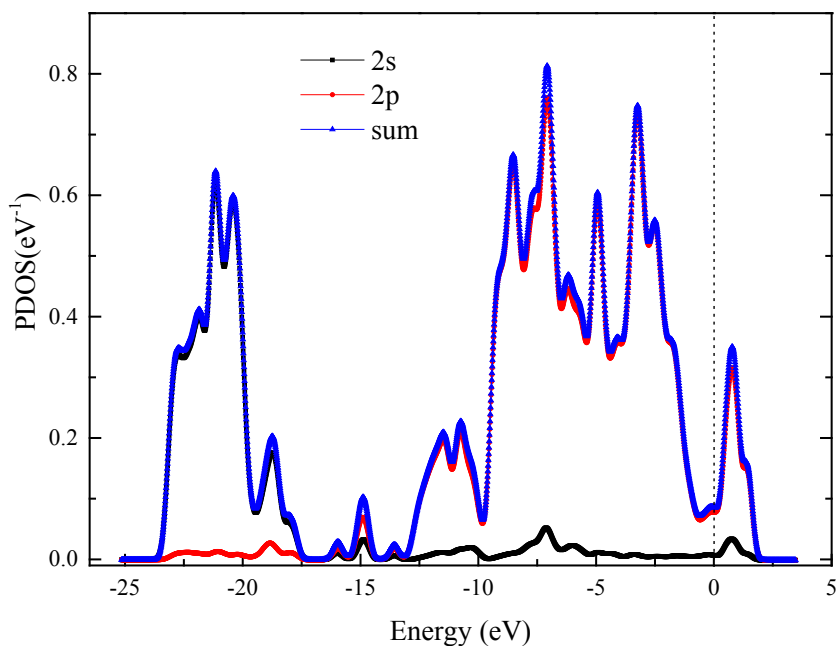


Fig.6-4 PDOS of each Element

From the partial DOS of each element shown in Fig. 6–4, it is found that there is mainly a contribution of O 2s states for the energy range of -25–20.5 eV and C 2p states for energy range from -15 to 0 eV and 0-5eV, the PDOS of three metal elements are as follow: In 4d states for the energy range of -13.5–-11.5 eV, In 5s states for the energy range of -10–-7.5 eV; Ga 4p states for the energy range of -20–-17.5 eV, Ga 4s states for the energy range of -15–-12.5 eV, Ga 3d states for the energy range of -15–-12.5 eV; Zn 4s states for the energy range of -22.5–-20.5 eV, Zn 4p states for the energy range of -20–-17.5 eV, Zn 3d states for the energy range of -17.5–-14.5 eV. Particularly, the valence-band is made up from O 2s, In 4d, Zn 3d and Ga 3d. The conductive-band is made up from O 2p, In 4d, Zn 4s and Zn 3p. The total DOS at Fermi level mainly originates from Zn or M (M =In, Ga) 3d states. It shows the biggest of the others because of metal *nd* states. Meanwhile, strong p-d hybridization can be seen between Zn- O and M ((M =In, Ga))-O atoms. Thus, there are covalent bonding contributions between Zn-O and M-O atoms. In the previous work, the electronic structure of InGaZn₂O₅ and InGaZn₃O₇ phases is affected by the content of Zn element. This fact is has been proved by experiment in chapter 3 and chapter 4 in this thesis.

6.2.4 Spectroscopic Analysis

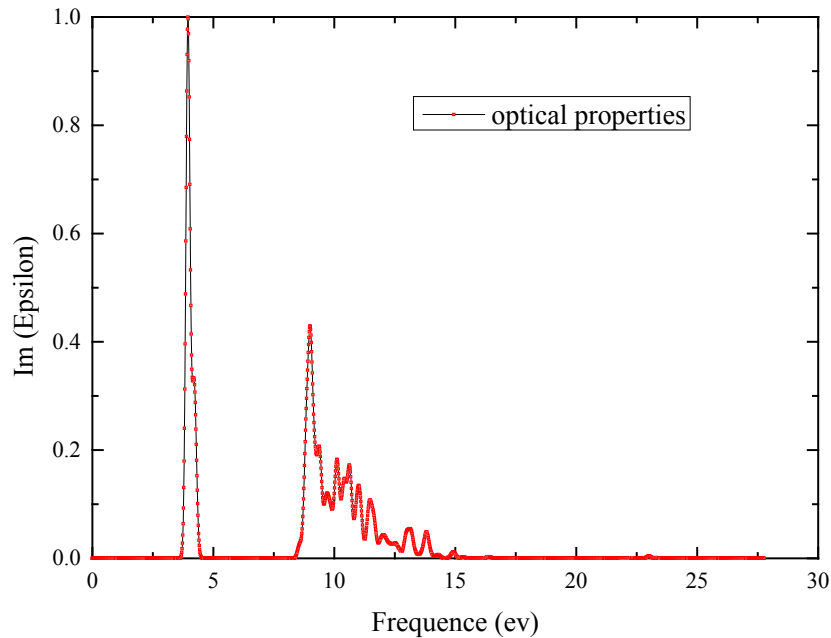


Fig.6-5 Optical Properties' of GaInZn₂O₅

The optical property of InGaZn₂O₅ is as show in Fig.6-5. The analysis of the optical functions of solids helps to give a better understanding of the electronic structure. The complex dielectric function is defined as:

$$\varepsilon(\omega) = \varepsilon_1(\omega) + i\varepsilon_2(\omega), \quad (6-1)$$

$$N(\omega) = n(\omega) + ik(\omega), \quad (6-2)$$

$$\varepsilon(\omega) = N^2(\omega). \quad (6-3),$$

Here ω is the angular frequency. The real part $\varepsilon_1(\omega)$ of the dielectric function can be obtained by the Kramers–kroning transform which links the real and imaginary parts. We have calculated the absorption, refractive index and other optical properties, which can be derived from the dielectric function. Fig. 6-5 shows the optical properties, absorption positions in the energy range ~ 3.1 eV due to its semiconductor nature. Since the material has wide-band gap as evident from band structure, the photoconductivity starts with zero photon energy for both polarization vectors.

Acknowledgements

The coming summer season marks the terminus of my two years journey of study abroad and I would like to take this opportunity to thank all those who have helped and supported me in completing the academic life.

First and foremost, I would like to give my utmost gratitude to my supervisor, Professor Toshihiro Moriga, for his encouragement, patience and selflessness guidance throughout the entire duration of this research work. Moreover, his active attitude and spirit in life also have a great influence on my personality. The mountain climbing and look around in the beautiful landscape of Tokushima together are also the best memories, so I need to cherish forever.

I would like to express my deepest thanks to Professor Youlong Xu in Xi'an Jiaotong University, my supervisor, for introducing me into the exciting research world and providing me the hard-won chance to study abroad in Japan. Without his supports, I will not get such an opportunity to gain valuable experience.

I would also like to express my heartfelt thanks to Associate Professor: Kei-ichiro Murai, Geoffrey I.N. Waterhouse, and Aparna Koinkar.

Many thanks extend to the students: Masaya Nishimoto, Toru Fujii, Katsuya Nakata, Kouji Ikenaga, Narendra Sarda, Yuma Ogita, Ken Nagai, Masaki Fujikawa, Hirata Kento, Minami Omune, Hiroshi Fujigaki, Yutaro Nomura, Takanori Hayashi, Takeuchi Yuta, Satoshi Kataoka, and Takahasi Masaru in Moriga group, for their help and patience in my research and life, especially at the time that I can't speak any Japanese.

I would especially like to thank my good brothers: Guodong Zhang, Huijun Liu, Liuan Li and Ke Shang, Jun Ding in the international house of Tokushima University for the precious time spent together in an alien land.

Last and certainly not the least, I am forever indebted to my parents and family, who have been supporting me through all of the accomplishments of my academic life.

Their indefinite love has made the things different in every aspect of my life.

Biography

Xinzhi Wang was born in Baoji City, Shaanxi province, China on 10th. Oct. 1979.

2001.09-2005.07: he graduated with a Bachelor of Science degree in chemistry from Northwest University, China.

2005.09-2008.07: he was recommended to complete his Master of Science degree in physics chemistry from Northwest University, China.

2008.09-2011.03: he served as an analysis engineer in Institute of Chemistry Chinese Academy of Sciences.

2011.09-2017.06: he has been engaged in the semiconductor physical in Xi'an Jiaotong University

2013.10.-2015.09: he has been studied as Double Degree student in chemistry in Tokushima University , Tokushima, Japan.

He has received the following awards:

1. 日本学生支援機構(JASSO) 奨学金 (2013.10-2014.09)

2.Nichia Scholarship Certificate, Tokushima University (平成26年度徳島大学工学部日亜特別待遇奨学金).(2014.10-2015.09)

Publication list

Scientific Papers

1. Xinzhi WANG, Masaya NISHIMOTO, Toru FUJII, et al. Deposition of IGZO or ITZO thin films by co-sputtering of IZO and GZO or ITO targets, *Advanced Materials Research*, 2015, Vol. 110, pp 197-202
2. Xinzhi WANG, Masaya NISHIMOTO, Toru FUJII, et al. Preparation and characterization of InGaSnO thin film by DC sputtering. *Materials Research Bulletin*. (In pressing)
3. Liuan Li, Xinzhi Wang, Jin-Ping Ao. NiO/GaN Heterojunction Diode Deposited by Magnetron Reactive Sputtering, *Journal of Vacuum Science & Technology A*, 2016. 34 (2).
4. Y.F. Li, B. Xiao, L. Sun, X.Z.Wang, Y.M. Gao and Y.H. Cheng, Phonon Spectrum, IR and Raman Modes, Thermal Expansion Tensor and Thermal Physical Properties of Ordered MAX phase M_2TiAlC_2 (M=Cr, Mo, W), *computational materials science*, 2017, 134:67–83
5. Jianqiang Wang, Ziping Li, Xinzhi Wang, et al. Cyclohexane-Fused Pyridine Derivatives with Photophysical Properties: Synthesis by “Three-Component” Domino Reaction and Structural Optimization by DFT Calculations, *Heterocycles*, 2015, Vol .91, No. 1, pp.49-63

Conference and conference paper/poster

1. Xinzhi WANG, Masaya NISHIMOTO, Toru FUJII, Kikuo TOMINAGA, Kei-ichiro MURAI, Toshihiro MORIGA and Youlong XU, 7th International Conference on Advanced Materials development and Performance. Deposition of IGZO or ITZO thin films by co-sputtering of IZO and GZO or ITO targets, 2014, July.17-20, Korea Maritime and Ocean University, Busan, Korea
2. Xinzhi WANG, Katsuya NAKATA, Kei-ichiro MURAI, Toshihiro MORIGA, Youlong XU. International Forum on Advanced Functional Materials and Polymer

Materials, Preparation and characterization of IGTO thin film by DC sputtering. May 30th, 2015, Qingdao, China,

3. Katsuya Nakata, Xinzhi Wang, Toru Fujii, Keichiro Murai and Toshihiro Moriga. 2015, March.9th. The University of Tokushima, Japan. International Forum on Advanced Technologies, Preparation of sintered compacts and sputtered films with IGTO T-phase structure as transparent conductor,